

CHARACTERISTICS OF FLOW IN WET CONICAL SPOUTED BEDS OF UNEQUAL-SIZED SPHERICAL PARTICLES

M. S. Bacelos, M. L. Passos and J. T. Freire*

Departamento de Engenharia Química, Centro de Secagem de Pastas, Suspensões e Sementes,
Universidade Federal de São Carlos, Fax: +(55) (16) 3351-8266, Rod. Washington
Luiz km 235, Cx.P 676, CEP: 13565-905, São Carlos, SP, Brazil
E-mail: freire@power.ufscar.br

(Received: January 16, 2006 ; Accepted : September 26, 2007)

Abstract - Interparticle forces, developed in wet spouted beds composed of a mixture of spherical particles with different size distributions, intensify particle segregation mechanisms interfering in gas distribution inside the bed and, consequently, in the spouting flow characteristics. Therefore, this paper is aimed at describing the effect of interparticle forces on the air-solid flow distribution in conical spouted beds of unequal-sized particles coated by a thin glycerol film. Experimental results show that both the minimum spouting airflow rate and the minimum spouting pressure drop decrease as the amount of glycerol added to the bed increases. In addition, simulated results of the annular air velocity along the bed height showed that, at the base of the column, the radial component of the inertial force is high enough to break liquid bridges between particles and carry these particles out along the spout. Moreover, as the glycerol concentration increases, the spout diameter increases along the bed height. Such changes in the air-solid flow can maintain the spouting regime for higher glycerol concentrations as shown by experimental data.

Keywords: Wet conical spouted bed; Minimum spouting conditions; Cohesive forces; Unequal-sized spherical particles.

INTRODUCTION

Over the fifty years since its discovery, researchers have tried to apply the spouted bed technique in many industrial processes, such as pneumatic conveyance (Ferreira and Freire, 1992; Ferreira and Narimatsu, 2001; Costa et al., 2004); catalytic polymerization (Bilbao et al., 1987); pyrolysis of sawdust (Aguado et al., 2000); drying of grains (Mathur and Gishler, 1955; Mathur and Epstein, 1974; Devahastin et al., 1998), pastes or suspensions (Pham, 1983; Barret and Fane, 1990; Passos et al., 1997; Correa et al., 2000, 2004a,b; Spitzner Neto et al., 2001; Souza and Oliveira, 2005; Cordeiro and Oliveira, 2005); coating seeds (Duarte et al., 2004) and tablets (Publio and Oliveira, 2004); producing fuel powders (Passos et al., 2004),

pharmaceutical powders (Jono et al., 2000) and fertilizers (Ayub et al., 2001).

In small-scale production, the conical spouted bed dryer is pointed to as a more promising technique for processing viscous and thermal sensitive suspensions (Spitzner Neto et al., 2002; Trindade et al., 2004; Bacelos et al., 2005, 2007) than other techniques, such as fluidization (Daleffe and Freire, 2004) or spray-drying (Birchal et al., 2005, 2006).

In conical spouted beds, high rates of heat and mass transfer coupled with the intensive attrition between particles induce high shear rates in the thin suspension layer that coats particles, reducing its apparent viscosity and making feasible the drying operation for powder production (Passos et al., 2004). Moreover, in the drying of pastes or suspensions some problems that reduce powder

*To whom correspondence should be addressed

production, such as particle agglomeration and particle adhesion to dryer walls, must be overcome. Thus, in order to produce optimum values of either paste or moisture material content in the bed, Spitzner Neto et al. (2001, 2002) verified that monitoring the bed suspension feed can control these conditions. Passos et al. (2004) proposed and proved that the problem of particle agglomeration can be well overcome by feeding the suspension into the conical spouted bed of inert particles intermittently under a rigid control of outlet air temperature. For a pseudoplastic suspension, such as black liquor, this rigid control maintains the liquor viscosity low enough to make feasible the continuous production of powdery fuel from eucalyptus and bamboo black liquor.

In spite of the many potential applications of the conical spouted bed technique, as pointed out in the literature (Mathur and Epstein, 1974; Passos et al., 1997; Devahastin et al., 1998) the thermal performance of air is still low for industrial applications. Recently, Fernandes and Correa (2005) showed how to recycle the exhaust gas and recover its sensitive heat in order to increase the energy efficiency of the operation of drying of pastes in conical spouted beds.

Experimental results together with validated models to predict momentum, heat and mass transfer in porous media allow researchers to simulate optimum routes for drying and powdering suspensions. Therefore, efforts have been made to describe fluid flow characteristics in conical spouted beds (Charbel et al., 1999; Spitzner Neto et al., 2001; Costa Jr. et al., 2004; Duarte et al., 2005; Bacelos et al., 2005) as well as drying mechanisms (Passos et

al., 2004; Trindade et al., 2004; Costa Jr. et al., 2006).

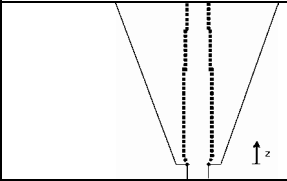
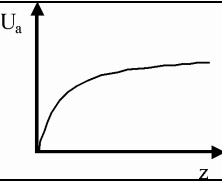
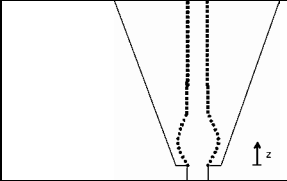
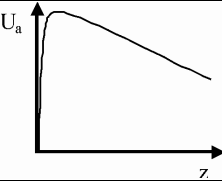
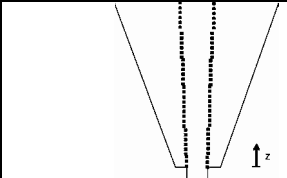
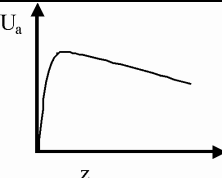
Initially, Costa Jr. et al. (2001) proposed a simulator predicting the drying of diluted Newtonian suspensions in conical spout-fluid beds, ignoring the effect of interparticle forces. This simulator consists of three interactive modules: gas flow (module 1), solid flow (module 2) and drying (module 3). According to these authors, the main feature of modules 1 and 2 is to predict gas and solids flow behavior as a function of the spout formation mechanism, which is specified by range of parameter (A) as shown in Table 1. This parameter (A) relates the minimum inlet energy required to form the spout to the minimum frictional energy lost to maintain the spout throughout its area (Littman and Morgan, 1988):

$$A = \frac{\rho_g U_{mf} U_T}{(\rho_s - \rho_g) g d_i} \quad (1)$$

where ρ_g and ρ_s are respectively the gas and solid density, U_{mf} is the minimum fluidization gas superficial velocity, U_T is the terminal particle velocity, g is gravity force and d_i is the inlet nozzle diameter.

Output variables from module 1 and module 2 enter into module 3, where mass and energy balance equations are developed for solids, gas and suspension. These equations are solved along the bed height and together with the drying kinetics correlation for the suspension. These three modules supply all data needed for describing the operation of drying diluted suspension.

Table 1: Gas flow characteristics as a function of bed failure mechanisms, expressed by range of parameters A (Costa Jr. et al., 2001).

| Range of A | Spout termination mechanism | Spout shape | Air distribution in the annulus |
|--------------------------|---|---|---|
| $A > 0.02$ | Fluidization of the top of the bed |  |  |
| $0.014 \leq A \leq 0.02$ | Transitional |  |  |
| $A < 0.014$ | Degeneration of spout into slugs at the base of the bed |  |  |

Charbel et al. (1999) showed that the changes in gas-flow characteristics are related to the failure mechanism of the bed and depend on geometric parameters alone. Moreover, these authors verified that for each specified range of parameter A presented in Table 1, there is a relation between parameter A, type of spout formation mechanism, spout shape and gas flow behavior. Such a relation was considered in the simulator proposed by Costa Jr. et al. (2001), which estimates either spout diameter or gas superficial velocity as a function of axial direction for different ranges of parameter A.

Trindade et al. (2004) proposed a methodology to introduce into this simulator the effect of interaction forces between inert particles coated by suspension. This technique is based on correlations developed by Passos and Mujumdar (2000), which consider that the effect of interparticle forces can be quantified by two specific curves: (Q_{mj}/Q_{mj0}) vs. $p_1 = \epsilon(1-\epsilon_{ag})/\epsilon_{ag}$ and $(\Delta P_{mj}/\Delta P_{mj0})$ vs. $p_2 = p_1\phi/d_p$. Then, by changing the type and amount of suspension injected into the bed of inert particles, the minimum spouting gas flow rate (Q_{mj}) changes in relation to the one obtained in the bed of dry particles (Q_{mj0}). Consequently, this induces changes in the minimum spouting pressure drop (ΔP_{mj}) in relation to that obtained in the bed of dry particles (ΔP_{mj0}). The type of interaction forces is directly related to the suspension properties, but the strength of these forces depends on the thickness of the suspension layer that covers the particle surface as well as the bed failure mechanism during spout formation (Charbel et al., 1999).

As reported in the literature, changes in the behavior of fluid dynamic variables, such as ΔP_{mj} and Q_{mj} , are associated with gas flow rate crossing the spout-annulus interface. Moreover, any change in the inlet gas flow rate produces modifications in the shape of spout diameter along the bed height. Therefore, Trindade et al. (2004) used two corrective functions with adjustable parameters to modify the simulator. The first one, f_1 , depends on p_1 and z/H and is applied to the spout-diameter model equation.

The second corrective function, f_2 , depends on p_2 and z/H (in the same way that f_1 depends on p_1 and z/H) and is applied to the gas flow rate crossing the spout-annulus interface. These authors tested this methodology to include the effect of interparticle forces between polypropylene particles coated by Eucalyptus black liquor in a conical spouted bed with $A > 0.02$. Based on photographic results, they showed that the spout closes as the amount of suspension injected into the bed is increased. A simulator using optimization routes to define either the type of these corrective functions (f_1, f_2) or their adjustable parameters can effectively predict this behavior.

Recently, Costa Jr. et al. (2006) have applied this methodology to describe flow characteristics of a conical spouted bed of spherical glass beads at $A = 0.015$ (transitional bed failure mechanism $0.014 < A < 0.02$) during the drying of egg emulsion. Their simulated results show good agreement with the characteristics of bed behavior reported during experiments.

However, for more general purpose, this modified simulator should be applied for other column dimensions (at least $A < 0.014$), unequal-sized particles and different suspensions. Note that wet beds of unequal-sized particles may simulate quite well the effect of interparticle binding forces on the drying of suspension since, in practice, the agglomeration phenomena should cause nonuniformity in the equal-sized particle packing interfering with gas-solid flow characteristics. Using unequal-sized particles as inert particles, such interference is intensified.

Therefore, as a first step, this paper is aimed at applying this methodology to describe the effect of interparticle forces on airflow distribution in a wet conical spouted bed of spherical unequal-sized particles. To simulate the effect of a highly viscous suspension, glycerol, a nonvolatile liquid, is used. As shown in Table 2, this Newtonian liquid has physical properties similar to those of pseudoplastic suspensions without the effect of the moisture concentration on these properties.

Table 2: Glycerol properties compared to those reported for egg emulsion and eucalyptus black liquor.

| Properties | Glycerol (This work) | Egg emulsion (Costa et al., 2006) | Eucalyptus black liquor (Passos et al., 2004) |
|--|---------------------------|--|--|
| Density ρ_{sup} (kg/m ³) | 1258 | 1040-1080 for $C_{ss}=30-60\%$ | 1050-1600 for $C_{ss}=10-78\%$ |
| Superficial tension σ_1 (N/m) | 0.06 at $T=60^\circ C$ | 0.075-0.140 for $C_{ss}=0-45\%$ at $T=60^\circ C$ | 0.022-0.034 for $C_{ss}=5-60\%$ at $T=90^\circ C$ |
| Viscosity μ_{susp} (Pa.s) | 0.1 at $T=60^\circ C$ | — | — |
| and Rheological Behavior | Newtonian behavior | at $C_{ss} = 0-44\%$ Newtonian behavior at $C_s = 44-99\%$ Pseudoplastic behavior | at $C_{ss} = 10-30\%$ Newtonian behavior at $C_{ss} = 35-65\%$ Pseudoplastic behavior |

INTERPARTICLE FORCES IN CONICAL SPOUTED BEDS OF UNEQUAL-SIZED PARTICLES

The spouting regime in conical spouted beds is achieved as the inertial force from the inlet gas jet is high enough to break the packed bed structure, usually in the central column axis, and to carry out particles, forming a fountain above the bed. This means that this inertial force on particles must overcome gravity and any other interparticle force. Therefore, due to the action of the inertial inlet gas force, a continuous and cyclic particle movement is established inside the column, characterizing the spouting regime. This regime consists of a central core dilute phase (called spout) moving upward; a fountain, formed of particles that leave the spout and rain back onto the annulus surface; and an annular dense phase, characterized by the sliding motion of particles in countercurrent to the gas flow.

For conical spouted beds, San José et al. (1995) presented the velocity vector map as it is schematically shown in Figure 1. At a given axial bed position (z), at the spout, the air velocity vectors (i.e., the interstitial ones) present a quasi-flat profile with r -direction and become an approximately parabolic profile with r -direction at the annulus. In addition, at a given radial bed position (r), the velocity vectors decrease with an increase in z -direction. Thus, the highest radial and axial velocity components are seen at the bottom of the bed, as shown in Figure 1.

According to Charbel et al. (1999), especially for the conical spouted bed used in this research with $A = 0.015$ (i.e., in a range of $0.014 < A < 0.02$), there is a characteristic flow behavior, which was previously

shown in Table 1. Such behavior can be explained by the air inertial force attained in the spouting regime. The air injected vertically through an inlet nozzle diameter flares out into the annulus as it travels upward (i.e., at air velocity $v = 1.1v_{mj}$, about 40-54% of the air injected into the bed crosses into the annulus region [see Mathur and Epstein, 1974; Charbel et al., 1999]). At the bottom of the bed, the airflow behavior is due to the contribution of both radial and axial air velocity components in the inertial force. Thus, the axial inertial force component shears the particle layer at the spout-annulus interface and the radial one presses the assembly firmly, enlarging the spout region. On the other hand, as the air travels upward in the bed carrying particles, it loses energy by friction with solids, decreasing its inertial force components. This can be proved by the decrease in magnitude of air velocity vectors as the z -direction is increased (see Figure 1).

Moreover, as a conical spouted bed characteristic, the annulus area increases with the increase in bed height, inducing higher resistance to air crossing this interface in the direction of the annular region. Therefore, at a given bed axial position (z), enlargement of the spout starts to decrease, so that, it narrows back. Thereafter the spout remains practically constant close to the top of the bed as shown in Table 1. In addition, note that, as liquid is added to the bed, this spout enlargement with the axial direction becomes more pronounced (see point **b** in Figure 2). Such behavior is strongly dependent on interparticle forces developed between wet particles under the minimum spouting condition. These forces interfere with the magnitude of inertial force at the base and top of the column (Bacelos et al., 2007).

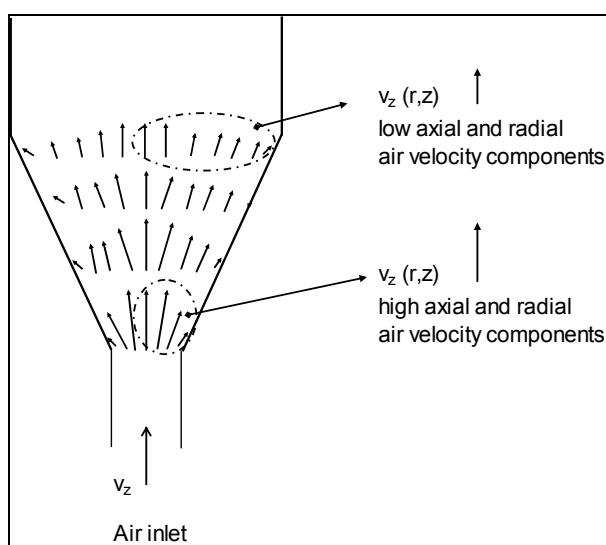


Figure 1: Schematic representation of the velocity maps for conical spouted beds. With specification as $\alpha = 72^\circ$; $d_b = 0.04$ m; $d_p = 3$ mm; $H = 0.22$ m and at $v = v_{mj}$. San José et al. (1995).

In conical spouted beds of unequal-sized particles, the particle size segregation can occur as schematized in Figure 2. This phenomenon is predominantly governed by the action of the particle inertia and the gravitational force. Note that, in the fountain region, particles move approximately in parabolic trajectories before falling onto the top of the annular region. As shown in Figure 2, the smaller particles reach the top of the annulus at regions near the column wall as they travel longer radial distances than those traveled by the coarser ones. This solids flow behavior in the bed explains the formation of liquid bridges between particles of different sizes. At the spout-annulus interface, liquid bridges exist between coarser particles; however, as liquid moves radially outward in the bed, liquid bridges can also occur between unequal-sized particles and in regions close to the column wall, liquid bridges between smaller particles can be found.

As reported in the literature (see Seville et al., 2000; Hotta et al., 1974), forces on bridges such as capillary and boundary forces (F_{cb}), increase with the increase in the particle diameter. For two given unequal particles on the bridge, F_{cb} is stronger the lower the difference between particle diameters

(Bacelos et al., 2007). The viscous force on particle (F_v) depends on particle size as well as the magnitude of axial air velocity, as this can induce a relative movement between particles on bridges. Thus, due to the particle size and air-flow behavior in this conical spouted bed of unequal-sized particles shown in Figure 2, the total interparticle force ($F = F_v + F_{cb}$) increases radially from the column wall to the spout-annulus interface and axially from the top to bottom of the bed.

Finally, as shown in Figure 2, concentrations of coarser particles (i.e., those of highly cohesive liquid bridges) are higher at the spout-annulus interface, and then a greater inertial force is required from the air jet to break off these liquid bridges. Consequently, an increase in minimum spouting velocity is required to maintain the spouting regime. As noted, higher interparticle forces are achieved at the spout-annulus interface, increasing bed resistance to air crossing this interface into the annulus region. Therefore, the airflow into the spout is eased (i.e., less particle cross flow from annulus to spout), decreasing the minimum spouting pressure drop significantly for distributions containing a high weight fraction of coarse particles.

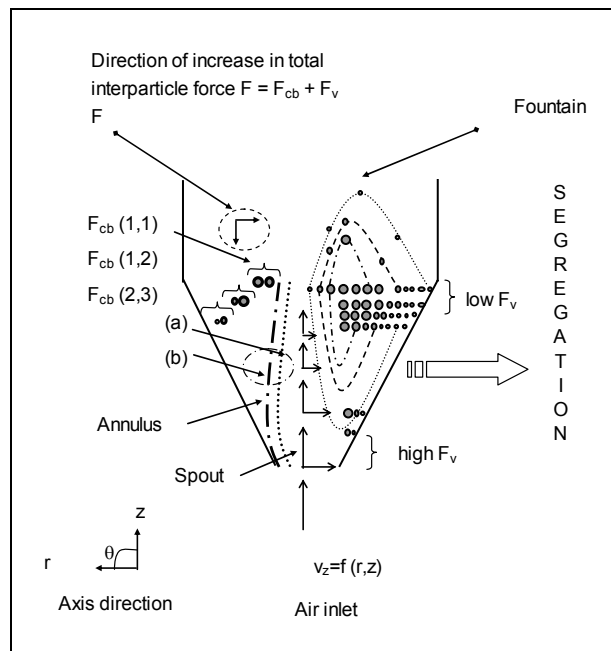


Figure 2: Profile for particle segregation and interparticle forces in conical spouted beds with particle mixtures. $F = F_{cb} + F_v$.

EXPERIMENTAL METHODOLOGY

Material and Apparatus

Table 3 shows the type and dimensions of the conical spouted bed column and inert particles used in this work in comparison to those used by Trindade et al. (2004) and analyzed by Costa Jr. et al. (2006).

As noted in Table 3, the inert particles are a mixture of spheres with three different diameters (small – $d_{pS} = 2.18$ mm, medium – $d_{pM} = 2.58$ mm and large – $d_{pB} = 3.67$ mm) in the following mass proportions: 22 % small, 36 % medium and 42 % large. This results in a flat size distribution (i.e., a linear relationship between particle mass fraction and diameter) with a Sauter diameter (average diameter)

equal to that of the medium-sized particles ($d_s = 2.58$ mm), as reported by Bacelos and Freire (2005, 2006).

Figure 3 shows the detailed experimental apparatus used in this work. This comprises a conical spouted bed with the dimension specified in Table 3, an air compressor to blow air into the bed, a flow rate Venturi meter to measure the air inlet flow rate and manometers to measure the pressure drop along the bed. In addition, pressure transducers are used to capture analogical pressure signals of both bed and flow rate Venturi meter. Data are logged and processed by a supervisory system, which consists of a conditioning module, an acquisition board and software developed in the graphic program language, using Labview 7.0 by National Instruments.

Table 3: Data information analyzed in this present work.

| Reference | Apparatus | Measured variables | Particle properties |
|---------------------------|---|--|---|
| (This work) | Conical SB $d_c = 0.30$ m $d_b = 0.06$ m $d_i = 0.05$ m $\alpha = 60^\circ$ | ΔP vs. Q $M = 7$ kg $H = 0.185$ m $T_{gi} = 60^\circ\text{C}$ $0 \leq v_l/v_p \leq 0.008$ $A = 0.0150$ | GB (glass beads) $d_p = d_{\text{sauter}} = 2.58 \times 10^{-3}$ m; $\phi = 1$ $\rho_s = 2490$ kg/m ³ $\epsilon_{a0} = 0.39$ Flat mixture: (distribution) $d_{pS} = 2.18 \times 10^{-3}$ m $X_{pS} = 22$ $d_{pM} = 2.58 \times 10^{-3}$ m $X_{pM} = 36$ $d_{pB} = 3.67 \times 10^{-3}$ m $X_{pB} = 42$ |
| (Costa Jr. et. al., 2006) | Conical SB $d_c = 0.30$ m $d_b = 0.06$ m $d_i = 0.05$ m $\alpha = 60^\circ$ | ΔP vs. Q $M = 9.35$ kg $H = 0.205$ m $T_{gi} = 60^\circ\text{C}$ v_l/v_p : 0 to 0.21 Q_{sup} : 0 to 2.66 L/h $A = 0.0145$ | GB (glass beads) $d_p = 2.6 \times 10^{-3}$ m; $\phi = 1$; $\rho_s = 2490$ kg/m ³ ; $\epsilon_{a0} = 0.40$ |
| (Trindade et al., 2004) | Conical SB $d_c = 0.30$ m $d_i = 0.026$ m $d_b = d_i$ $\alpha = 60^\circ$ | ΔP vs. Q $M = 2$ kg $H = 0.197$ m, $v_l = 0$ to $32 \cdot 10^{-3}$ L $A > 0.020$ | PP (polypropylene particles) $d_p = 4.02 \times 10^{-3}$ m; $\phi = 0.92$; $\rho_s = 867$ kg/m ³ ; $\epsilon_{a0} = 0.38$ |

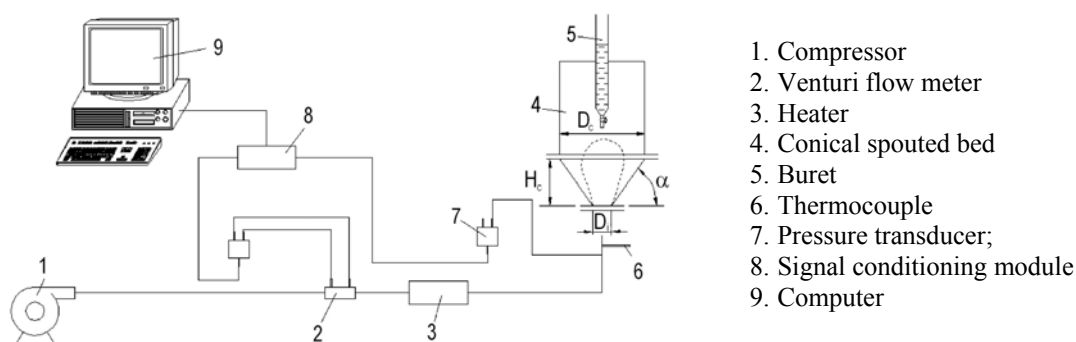


Figure 3: Schematic representation of experimental apparatus.

Experimental Procedure

Glycerol, used to simulate the presence of paste or suspensions in the bed, creates the cohesion between inert particles. A gradual buret is employed to add a known volume of glycerol to the bed, which is already in stable spouting regime. The addition of liquid under this condition assures a good homogeneity for liquid distribution on inert particles. For each given experimental condition, a measuring tape (in millimeters) fixed to the column wall is used to measure bed height. Thus, at a given glycerol concentration, the overall bed porosity, ϵ_a , in the annular region is determined. The dry-based bed porosity in the annulus region, ϵ_{ag} , is obtained by subtracting (v_l/v_{bed}) from the ϵ_a value.

Moreover, by keeping constant the mass of particles ($M = 7$ kg) and changing the glycerol concentration ($0 \leq v_l/v_p \leq 0.008$), the ΔP (pressure drop) vs. Q (airflow rate) curve is determined by decreasing Q for both dry and wet spouted beds. Based on these curves, the dimensionless ratios Q_{mj}/Q_{mj0} and $\Delta P_{mj}/\Delta P_{mj0}$ can be evaluated as a function of p_1 and p_2 .

Data Simulation

As experimental data on Q_{mj}/Q_{mj0} vs. p_1 and $\Delta P_{mj}/\Delta P_{mj0}$ vs. p_2 have been evaluated, the two corrective functions, f_1 and f_2 , are primarily chosen to be the same as those reported by Trindade et al. (2004):

$$f_i = 1 + \left(a_i \left[\frac{z}{H} \right] + b_i \right) p_i^{c_i} \quad i=1 \text{ to } 2 \quad (2)$$

As mentioned earlier, f_1 is applied to the spout diameter model equation and depends on p_1 and z/H and f_2 corrects the rate of airflow crossing the spout-annulus interface and depends on p_2 and z/H . Note that these two functions reach unit values in beds without suspension ($p_1 = p_2 = 0$). The procedure used to determine the six adjustable parameters, a_1, a_2, b_1, b_2 and c_1, c_2 , is the one proposed by Trindade et al. (2004) by minimizing the objective function defined as

$$f_{obj} = \sum_{i=1}^n \left[(DR_{Qi})^2 + (DR_{Pi})^2 \right] \quad (3)$$

with

$$DR_{Qi} = \frac{\left[Q_{mj} / Q_{mj0} \right]_{sim} - \left[Q_{mj} / Q_n \right]}{\left[Q_{mj} / Q_{mj0} \right]_{exp}}$$

$$DR_{Pi} = \frac{\left[\Delta P_{mj} / \Delta P_{mj0} \right]_{sim} - \left[\Delta P_{mj} / \right]}{\left[\Delta P_{mj} / \Delta P_{mj0} \right]_{exp}}$$

As suggested by these authors, the heuristic particle swarm optimization method, developed by Kennedy and Eberhart (1995), is chosen to optimize f_{obj} , as it is robust and efficient enough to guarantee that the adjustable parameter values obtained are those representative of the global minimum of the objective function.

RESULTS AND DISCUSSION

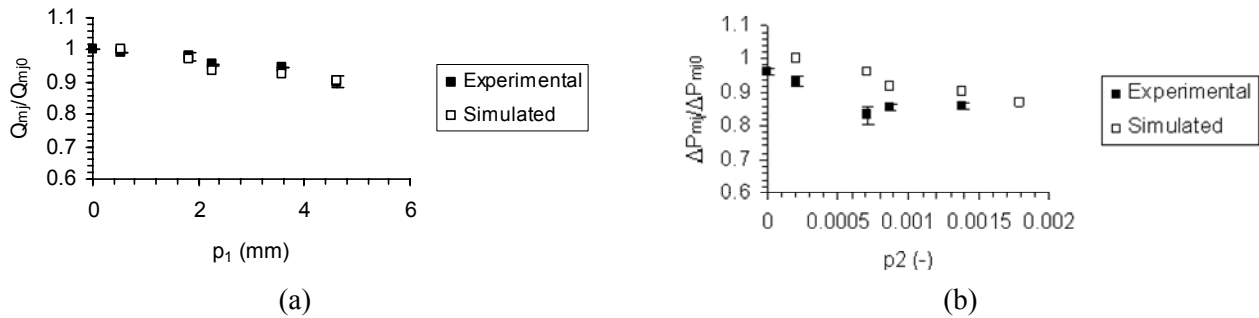
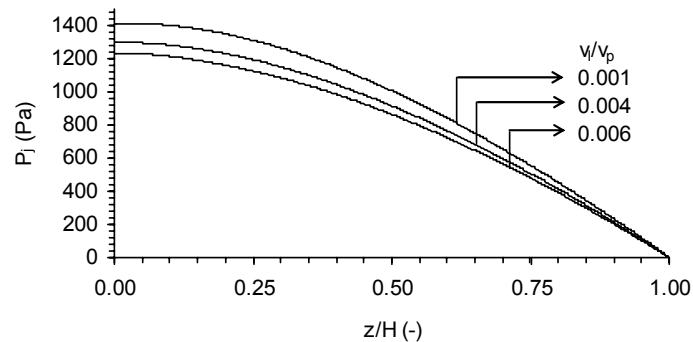
Table 4 shows the optimum values for the six parameters of the corrective functions in Equation 2. Based on these corrective functions of this work, the spouted bed operational variables, $Q_{mj}, \Delta P_{mj}, r_{mj}, U_a$ and P_j , can be simulated.

Figures 4a and 4b contain the experimental and simulated curves of operational spouted bed variables: the dimensionless minimum spouting flow rate ratio (Q_{mj}/Q_{mj0}) as a function of p_1 and the dimensionless minimum spouting pressure drop ratio ($\Delta P_{mj}/\Delta P_{mj0}$) as a function of p_2 . Based on the statistical analysis, the correlation coefficient (r) between these experimental and simulated data is 0.95 for the Q_{mj}/Q_{mj0} vs. p_1 curve and 0.85 for the $(\Delta P_{mj}/\Delta P_{mj0})$ vs. p_2 curve. This indicates that the model with the corrective functions in Table 4 is suitable for predicting quite well the Q_{mj}/Q_{mj0} vs. p_1 curve (mean error = 0.075 %) and reasonably well the $(\Delta P_{mj}/\Delta P_{mj0})$ vs. p_2 curve (mean error = -4.87 %). In addition, simulated errors are lower than experimental ones and acceptable statistically within the 95% of confidential interval. Therefore, one can conclude that this model with the corrective functions in Table 4 can be used to estimate the other flow variables as a function of the amount of glycerol in the bed.

Furthermore, as noted in Figures 4a and 4b, Q_{mj}/Q_{mj0} and $\Delta P_{mj}/\Delta P_{mj0}$ decrease with the increase in glycerol concentration (e.g. as p_1 and p_2 rise). The behavior of the Q_{mj}/Q_{mj0} curve is due to the formation of a liquid bridge and it increases as liquid binding forces between particles increase (Bacelos et al., 2007). These contribute to reduce the airflow rate crossing the spout-annulus interface and the particle motion in the annulus region. Thus, with the increase in glycerol concentration, a lower flow rate is needed to maintain the stable spouting regime as shown in Figure 4a. The trends of the $\Delta P_{mj}/\Delta P_{mj0}$ vs. p_2 curve can be explained by the increase in bed resistance to the passage of air through the spout-annulus interface in the presence of glycerol. This prevents part of the inlet air from crossing the interface, causing a reduction in bed pressure drop, as shown in Figure 4b. Therefore, the simulated $P_j(z)$ curves, shown in Figure 5, corroborate that the increase in glycerol concentration in the bed results in a decrease in gauge pressure at the spout-annulus interface. This indicates that less air crosses this boundary, in agreement with the $\Delta P_{mj}/\Delta P_{mj0}$ experimental trend behavior.

Table 4: Adjustable parameters obtained for two corrective functions, f_1 and f_2 .

| Parameters (Eq. 2) | Optimum values |
|----------------------------|----------------|
| $a_1 (\mu\text{m}^{-c_1})$ | 0.668 |
| $b_1 (\mu\text{m})^{-c_1}$ | 0.457 |
| $c_1 (-)$ | 1.670 |
| $a_2 (-)$ | -1.872 |
| $b_2 (-)$ | 1.520 |
| $c_2 (-)$ | -0.547 |
| $f_{\text{abi}} (-)$ | 0.0025 |

**Figure 4:** Experimental and simulated data for: (a) Q_{mj}/Q_{mj0} vs. p_1 ; (b) $\Delta P_{mj}/\Delta P_{mj0}$ vs. p_2 .**Figure 5:** Predicted pressure drop (P_j) along the spout-annulus interface as a function of z/H for a given paste concentration.

Figures 6a and 6b show the simulated profiles of the superficial air velocity in the annulus region, $U_a(z)$, and of the spout radius, $r_{mj}(z)$, as a function of glycerol concentration. In the range of $0 \leq v_1/v_p \leq 0.003$, these profiles are similar (not shown in Figs. 6a and 6b). Remarkable changes in the shape of the $U_a(z)$ curve are reported for $v_1/v_p \geq 0.004$. Note that, for a given glycerol concentration, $U_a(z)$ increases until reaching a maximum point close to $z/H < 0.125$ and thereafter begins decreasing at $z/H > 0.125$. Such behavior can be explained due to the enlargement of the spout radius (r_{mj}), in spite of the decrease in airflow rate from spout to annulus region. As shown in Figure 6b, the enlargement of spout radius (r_{mj}) is more pronounced from $z/H = 0$ to $z/H = 0.125$ than for the radius of the annular region. Moreover, this is a characteristic shape for conical spouted beds in a specific range of values for parameter A ($0.014 < A < 0.02$) presented in Table 1.

In spite of the fact that the $U_a(z)$ and $r_{mj}(z)$ profiles

are only simulated, these are in agreement with experimental trends reported for the values for the magnitude of liquid binding forces on bridges in conical spouted beds, as shown by the theory of cohesive forces. According to previous work (see Bacelos et al., 2007), the highest values for magnitude of these interparticle forces are found at the spout-annulus interface, as high values of viscous force are attained. Thus, only at the base of the column, the radial air velocity component has enough radial inertial force components to break off the liquid bridges between inert particles and carry them along the spout until reaching the bed surface. This behavior not only maintains the stable spouting regime, but probably enlarges the spout at the column base, as shown in Figure 6b. Moreover, in practical applications such as in coating of pellets and in drying of pastes, these expectations imply that particle agglomeration will start at $z/H > 0.125$, rather than at the column base, as this latter region has high values of U_a (see Figure 6a).

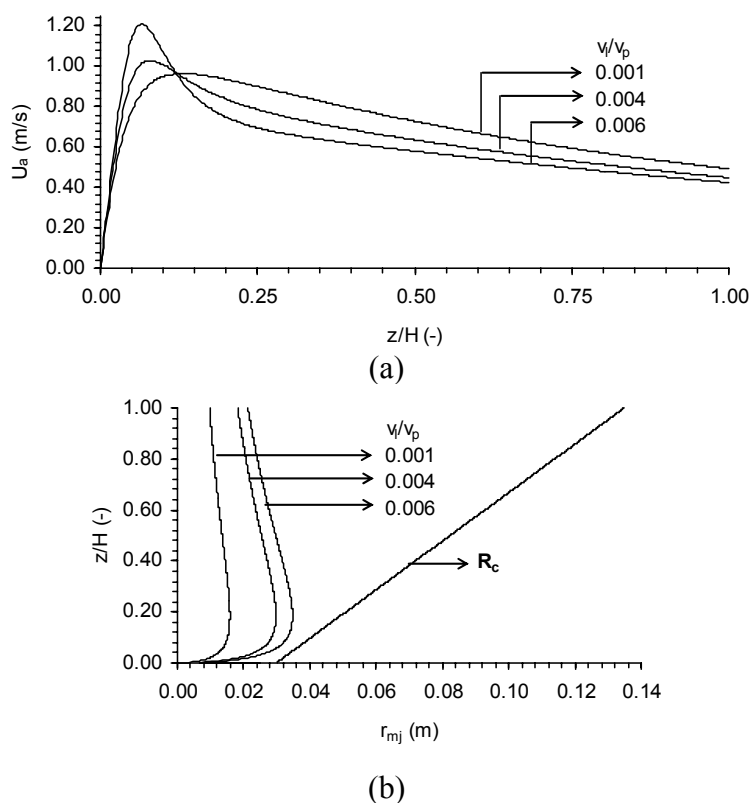


Figure 6: Predicted profiles for: (a) U_a vs. z/H as a function of v_l/v_p ; (b) r_{mj} vs. z/h as a function of v_l/v_p . R_c : Column radius.

By comparing this set of data to one reported for egg emulsion (see Costa Jr. et al., 2006), it can be noted that both sets of data are in agreement, as their spout radius increases with the increase in liquid concentration (glycerol or egg emulsion). This implies an increase in U_a at the column base and its reduction at the top (see Figure 6a), favoring particle agglomeration on the bed surface when the suspension is fed in the column top alone, as verified by Spitzner Neto et al. (2002) and by Bacelos et al. (2005).

On the other hand, data obtained here differ from those reported for eucalyptus black liquor (see Costa Jr. et al., 2006), as in this latter the spout radius narrows with the increase in concentration of eucalyptus black liquor added to the bed. As well, $U_a(z)$ becomes higher at top of the column than at the base. This indicates that particle agglomeration starts near the base of the column due to the reduction in $U_a(z)$ in this region, as pointed out by Trindade et al. (2004).

From these comparisons, one can see that the data presented are consistent with those for egg emulsion, which are obtained using the same equipment and inert particles. Consequently, the same transitional bed failure mechanism ($0.014 < A < 0.02$) is attained in both set of experiments, in spite of the differences

between these pastes. Thus, these sets of data differ from those on eucalyptus black liquor because, in the conical spouted bed of propylene inert particles, a different type of bed failure mechanism ($A > 0.02$) is obtained (see Table 1).

CONCLUSIONS

Based on these experimental data, one can note there is evidence showing that the behavior of conical spouted bed fluid dynamics changes significantly with mixture of particles, pastes or suspensions. As has been reported in the literature, such changes can be predicted well taking into account the effect of cohesive forces on the fluid dynamics behavior of the conical spouted bed. Therefore, the previous model has been demonstrated to be effective in predicting spouted bed operational variables. As shown in the Discussion section model prediction plays an important role in processes of drying of pastes. It allows determination of spout shape and annular superficial velocity profiles as a function of the suspension added to the spouted bed of inert

particles, and shows where in the bed particle agglomeration should start. This permits researchers to better understand both fluid dynamics and drying phenomena in wet spouted beds. Moreover, by comparing the model verification with the same bed and with different suspensions, it can be noted that the type of bed failure mechanism dictates the spouting airflow behavior in the wet bed, whereas the paste characterizes the magnitude of change in the operational spouted bed variables.

ACKNOWLEDGEMENTS

The authors express their gratitude to Conselho Nacional de Desenvolvimento Científico e Tecnológico (CNPq) for its financial support in carrying out this research, and especially to Coordenação de Aperfeiçoamento de Pessoal de Nível Superior (CAPES) and Fundação de Amparo à Pesquisa do Estado de São Paulo (FAPESP) for the D.Sc. and Ph.D. scholarship respectively awarded M. S. Babelos.

NOMENCLATURE

| | | |
|-----------------|---|----------------|
| a_i, b_i, c_i | adjustable parameters of f_i | (-) |
| A | parameter defined in Equation 1 | (-) |
| C_{ss} | solid concentration (% in mass) | (-) |
| d_b | diameter of the base of the column | m |
| d_c | diameter of the top of the column | m |
| d_l | inlet nozzle diameter | m |
| d_j | spout diameter | m |
| d_{mj} | spout diameter under minimum condition | m |
| d_p | particle diameter | m |
| d_{pl} | particle diameter of I-type particles (I = S – small; I = M – medium; I = B – large; see Tab.2) | m |
| d_s | Sauter particle diameter | m |
| e | suspension layer thickness = $(dp/2)[(1+V)^{1/3} - 1]$ | μm |
| f_i, f_{obj} | corrective and objective functions respectively | (-) |
| g | gravity acceleration | m/s^2 |
| H | bed height | m |

| | | |
|-----------|--|-----------------------|
| p_1 | $= e(1 - \epsilon_{ag}) / \epsilon_{ag}$ | μm |
| p_2 | $= e(\phi/dp)(1 - \epsilon_{ag}) / \epsilon_{ag}$ | (-) |
| Q_{mj} | gas flow rate at minimum spouting | m^3/s |
| Q_{mj0} | gas flow rate at minimum spouting for dry particles | m^3/s |
| r | correlation coefficient | (-) |
| r_{mj} | spout radius at minimum spouting (= $dm_j/2$) | m |
| R_c | column radius | m |
| U_a | gas superficial velocity in the annulus region | m/s |
| U_j | gas superficial velocity in the spout region | m/s |
| U_{mf} | gas superficial velocity at minimum fluidization | m/s |
| U_T | terminal particle velocity | m/s |
| v_{bed} | volume of the bed | m^3 |
| v_l | volume of suspension | m^3 |
| v_p | volume of particle | m^3 |
| X_{pl} | mass fraction of I-type particles (I = S – small, I = M – medium, I = B – large) | (-) |
| z | axial coordinate of the column | m |

Greek Symbols

| | | |
|------------------|--|-----|
| α | included column angle | 0 |
| ΔP_{mj} | minimum spouting pressure drop | Pa |
| ΔP_{mj0} | minimum spouting pressure drop for dry particles | Pa |
| ϵ_a | overall bed porosity | (-) |
| ϵ_{a0} | bed porosity in the annulus for dry bed | (-) |
| ϵ_{ag} | dry-based porosity in the annulus | (-) |

REFERENCES

- Aguado, R., Olazar, M., Bilbao, J. and Barona, A., Pyrolysis of Sawdust in a Conical Spouted bed Reactor. Yields and Product Composition, Ind. Eng. Chem. Res., 39, 1925 (2000).
- Ayub, G. C. E., Rocha, S. C. S. and Perrucci, A. L. I., Analysis of the Surface Quality of Sulphur-Coated Urea Particles in a Two-Dimension Spouted Bed, Brazilian J. Chem. Eng., 18, 1, 13-22 (2001).

- Bacelos, M. S. and Freire, J. T., Analysis of Spouting Regime Stability with Binary and Ternary Particle Mixtures, *Proceeding of Congresso Brasileiro de Sistemas Particulados (Enemp 2004)*, Uberlândia-MG, Brazil, 1 CD (2005)(In Portuguese)
- Bacelos, M. S. and Freire, J. T., Stability of Spouting Regimes in Conical Spouted Beds with Inert Particle Mixtures, *Ind. Eng. Chem. Res.*, 45, 2, 808-817 (2006).
- Bacelos, M. S., M. L. Passos and J. T. Freire. Effect of Interparticle Forces on the Conical Spouted Bed Behavior of Wet Particles with Size Distribution, *Powder Technol.*, 174, 3, 114-126 (2007).
- Bacelos, M. S., Spitzner Neto, P. I., Silveira, A. M. and Freire, J. T., Analysis of Fluid Dynamics Behavior of Conical Spouted Bed in Presence of Pastes. *Drying Technol.*, 23, 3, 427-453 (2005).
- Barret, N. and Fane, A., Drying of Liquid Material in a Spouted Bed. In *Drying '89*, eds. Mujumdar, A. S. and Roques, M. A., New York: Hemisphere Publishing Corporation, 415-420 (1990).
- Birchal V. S., Huang, L., Mujumdar, A. S. and Passos, M. L., Spray Dryers: Modeling and Simulation, *Drying Technol.*, 24, 3, 359-371 (2006).
- Birchal, V. S., Passos, M. L., Wildhagen, G. R. S. and Mujumdar, A. S., Effect of Spray-Dryer Operating Variables on the Whole Milk Powder Quality, *Drying Technol.*, 23, 3, 611-636 (2005).
- Bilbao, J., Olazar, M., Romero, A. and Arantes, J. M., Design and Operation of a Jet Spouted Bed Reactor with Continuous Catalytic Feed in the Benzyl Alcohol Polymerization, *Ind. Eng. Chem. Res.*, 26, 1297 (1987).
- Charbel, A. L. T., Massarani, G. and Passos, M. L., Analysis of Effective Solid Stresses in a Conical Spouted Bed, *Brazilian J. of Chem. Eng.*, 16, 433-449 (1999).
- Cordeiro, D. S. and Oliveira, W. P., Technical Aspects of the Production of Dried Extract of *Maytenus Illicifolia* Leaves by Jet Spouted Bed Drying, *International Journal of Pharmaceutics*, 299, 1-2, 115-126 (2005).
- Correa, N. A., Correa, R. G. and Freire, J. T., Adaptive Control of Paste Drying in Spouted Bed using the GPC Algorithm, *Brazilian J. Chem. Eng.*, 17, 639-648 (2000).
- Correa, N. A., Costa, C. E. S., Correa, R. G. and Freire, J. T., Control of Spouted Bed Dryers, *Can. J. Chem. Eng.*, 82, 3, 555-565 (2004a).
- Correa, N. A., Freire, F. B., Correa, R. G. and Freire, J. T., Industrial Trials of Paste Drying in Spouted Beds under QDMC, *Drying Technol.*, 22, 5, 1087-1105 (2004b).
- Costa, I. A., Ferreira, M. C. and Freire, J. T., Analysis of Regime Transitions and Flow Instabilities in Vertical Conveying of Coarse Particles using Different Solids Feeding Systems, *Can. J. Chem. Eng.*, 82, 48 (2004).
- Costa Jr., E. F., Cardoso, M. and Passos, M. L., Simulation of Drying Suspension in Spout-Fluid Beds of Inert Particles, *Drying Technol.*, 19, 1975-2001 (2001).
- Costa Jr., E. F., Freire, F. B., Freire, J. T., Passos, M. L. Spouted beds of inert particles for drying suspensions. *Drying Technol.*, 23, 3, 315-325 (2006).
- Costa Jr., E. F., Passos, M. L., Biscaia Jr., E. C. and Massarani, G., New Approaches to Solve a Model for the Effective Solid Stress Distribution in Conical Spouted Beds, *Can. J. Chem. Eng.*, 82, 539-554 (2004).
- Daleffe, R. V. and Freire, J. T., Analysis of Fluid Dynamics Behavior of Fluidized and Vibrofluidized Beds Containing Glycerol, *Brazilian J. Chem. Eng.*, 21, 1, 35-46 (2004).
- Devahastin, S., Mujumdar, A. S. and Raghavan, G. S. V., Diffusion-Controlled Batch Drying of Particles in a Novel Rotating Jet Annular Spouted Bed, *Drying Technol.*, 16, 3-5, 525-543 (1998).
- Duarte, C. R., Murata, V. V. and Barrozo, M. A. S., A Study of the Fluid Dynamics of the Spouted Bed using CFD, *Brazilian J. Chem. Eng.*, 22, 2, 263-270 (2005).
- Duarte, C. R., Neto, J. L. V., Lisboa, M. H., Santana, R. C., Barrozo, M. A. S. and Murata, V. V., Experimental Study and Simulation of Mass Distribution of the Covering Layer of Soybean Seeds Coated in a Spouted Bed, *Brazilian J. Chem. Eng.*, 21, 1, 59-67, (2004).
- Fernandes, C. F. and Correa, R. G., Analysis of Energy Efficiency of Drying of Pastes in Spouted Bed. *Proceeding of Congresso Brasileiro de Sistemas Particulados (Enemp 2004)*, Uberlândia-MG, Brazil, 1 CD (2005). (In Portuguese)
- Ferreira, M. C. and Freire, J. T., Fluid-Dynamics Characterization of Pneumatic Bed using a Spouted Bed Solid Feeding System, *Can. J. Chem. Eng.*, 70, 905 (1992).
- Ferreira, M. C. and Narimatsu, C. P., Vertical Pneumatic Conveying in Dilute and Dense-Phase Flows: Experimental Study of the Influence of Particle Density and Diameter on Fluid Dynamic Behavior, *Brazilian J. Chem. Eng.*, 18, 3, 221-232 (2001).
- Hotta, K., Takeda, K. and Iinoya, K., The Capillary Binding Force of a Liquid Bridge, *Powder*

- Technol., 10, 231-242 (1974).
- Jono, K., Ichikawa, H., Miyamoto, M. and Fukumori, Y., A Review of Particulate Design for Pharmaceutical Powders and their Production by Spouted Bed Coating, Powder Technol., 113, 3, 269-277 (2000).
- Kennedy, J. and Eberhart, R. C., Particle Swarm Optimization, International Conference on Neural Networks. Perth, Australia (1995).
- Littman, H. and Morgan, M. H., Transport Processes in Fluidized Beds, Elsevier, Amsterdam, 287 (1988).
- Mathur, K. B. and Epstein, N., Spouted beds. New York: Academic Press, Inc (1974).
- Mathur, K. B. and Gishler, P. E., Study of Application of the Spouted Bed Technique to Wheat Drying, J. Appl. Chem., 5, 624-636 (1955).
- Pham, Q. T., Behavior of Conical Spouted-Bed Dryer for Animal Blood, Can. J. Chem. Eng., 61, 3, 426-434 (1983).
- Passos, M. L., Massarani, G., Freire, J. T. and Mujumdar, A. S., Drying of Pastes in Spouted Beds of Inert Particles: Design Criteria and Modeling, Drying Technol., 15, 2, 605-624 (1997).
- Passos, M. L. and Mujumdar, A. S., Effect of Cohesive Forces on Fluidized and Spouted Beds of Wet Particles, Powder Technol., 110, 222-238 (2000).
- Passos, M. L., Trindade, A. L. G., d'Angelo, J. V. H. and Cardoso, M., Drying of Black Liquor in Spouted Bed of Inert Particles, Drying Technol., 22, 1041-1067 (2004).
- Publio, M. C. P. and Oliveira, W. P., Effect of the Equipment Configuration and Operating Conditions on Process Performance and on Physical Characteristics of the Product during Coating in Spouted Bed, Can. J. Chem. Eng., 82, 1, 122-133 (2004).
- San José, M. J., Olazar, M., Penas, F. J. and Bilbao, J., Segregation in Conical Spouted Beds with Binary and Ternary Mixtures of Equidensity Spherical Particles, Ind. Eng. Chem. Res., 33, 1838-1844 (1994).
- San José, M. J., Olazar, M., Peñas, F. J. and Bilbao, J., Correlation for Calculation of the Gas Dispersion Coefficient in Conical Spouted Beds, Chem. Eng. Sci., 50, 13, 2161-2172 (1995).
- Schubert, H., Capillary Forces: Modeling and Application in Particulate Technology, Powder Technol., 37, 105-116 (1984).
- Seville, J. P. K., Willet, C. D. and Knight, P. C., Interparticle Force in Fluidization: a Review, Powder Technol., 13, 261-268 (2000).
- Souza, C. R. and Oliveira, W. P., Spouted Bed Drying of Bauhinia Forficata Link Extract: The Effects of Feed Atomizer Position and Operating Conditions on Equipment Performance and Product Properties, Brazilian J. Chem. Eng., 22, 239-247 (2005).
- Spitzner Neto, P. I., Cunha, F. O. and Freire, J. T., The Influence of the Paste Feed in the Minimum Spouting Velocity, Brazilian J. Chem. Eng., 18, 243-251 (2001).
- Spitzner Neto, P. I., Cunha, F. O. and Freire, J.T., Effect of the Presence of Pastes in a Conical Spouted Bed Dryer with Continuous Feeding, Drying Technol., 20, 789-811 (2002).
- Trindade, A. L. G., Passos, M. L., Costa Jr., E. F. and Biscaia Jr., E. C., The Effect of Interparticle Cohesive Forces on the Simulation of Fluid Flow in Spout-Fluid Beds, Brazilian J. Chem. Eng., 21, 113-125 (2004).